This article was downloaded by: [Renmin University of China]
On: 13 October 2013, At: 11:07
Publisher: Taylor & Francis
Informa Ltd Registered in England and Wales Registered Number: 1072954 Registered office: Mortimer House, 37-41 Mortimer Street, London W1T 3JH, UK

Molecular Crystals and Liquid Crystals
Publication details, including instructions for authors and subscription information:
http://www.tandfonline.com/loi/gmcl20

Fabrication of Microstructures Containing High Refractive Index Materials by Two-Photon Lithography

Prem Prabhakaran [a b], Kyung-Kook Jang [a], Yong Son [c], Dong-Yol Yang [c] & Kwang-Sup Lee [a]

[a] Department of Advanced Materials, Hannam University, Daejeon, South Korea

[b] Laboratoire Interdisciplinaire de Physique (LIPhy), University of Grenoble, UJF-Baitment E45,140 rue de la Physique-BP 87, Saint Martin d' Hères, France

[c] Department of Mechanical Engineering, Korea Advanced Institute of Science and Technology, Daejeon, South Korea

Published online: 02 Sep 2013.

To cite this article: Prem Prabhakaran, Kyung-Kook Jang, Yong Son, Dong-Yol Yang & Kwang-Sup Lee (2013) Fabrication of Microstructures Containing High Refractive Index Materials by Two-Photon Lithography, Molecular Crystals and Liquid Crystals, 578:1, 4-18, DOI: 10.1080/15421406.2013.802960

To link to this article: http://dx.doi.org/10.1080/15421406.2013.802960

PLEASE SCROLL DOWN FOR ARTICLE

Taylor & Francis makes every effort to ensure the accuracy of all the information (the "Content") contained in the publications on our platform. However, Taylor & Francis, our agents, and our licensors make no representations or warranties whatsoever as to the accuracy, completeness, or suitability for any purpose of the Content. Any opinions and views expressed in this publication are the opinions and views of the authors, and are not the views of or endorsed by Taylor & Francis. The accuracy of the Content should not be relied upon and should be independently verified with primary sources of information. Taylor and Francis shall not be liable for any losses, actions, claims, proceedings, demands, costs, expenses, damages, and other liabilities whatsoever or howsoever caused arising directly or indirectly in connection with, in relation to or arising out of the use of the Content.

This article may be used for research, teaching, and private study purposes. Any substantial or systematic reproduction, redistribution, reselling, loan, sub-licensing, systematic supply, or distribution in any form to anyone is expressly forbidden. Terms &

Conditions of access and use can be found at http://www.tandfonline.com/page/terms-and-conditions

Downloaded by [Renmin University of China] at 11:07 13 October 2013

Mol. Cryst. Liq. Cryst., Vol. 578: pp. 4–18, 2013
Copyright © Taylor & Francis Group, LLC
ISSN: 1542-1406 print/1563-5287 online
DOI: 10.1080/15421406.2013.802960

Downloaded by [Renmin University of China] at 11:07 13 October 2013

Fabrication of Microstructures Containing High Refractive Index Materials by Two-Photon Lithography

PREM PRABHAKARAN,[1,2] KYUNG-KOOK JANG,[1] YONG SON,[3] DONG-YOL YANG,[3] AND KWANG-SUP LEE[1,*]

[1]Department of Advanced Materials, Hannam University, Daejeon, South Korea
[2]Laboratoire Interdisciplinaire de Physique (LIPhy), University of Grenoble, UJF-Baitment E45,140 rue de la Physique-BP 87, Saint Martin d' Hères, France
[3]Department of Mechanical Engineering, Korea Advanced Institute of Science and Technology, Daejeon, South Korea

Here we review our work on incorporating high refractive index inorganic materials into microstructures by two-photon lithography. We describe the direct writing of silver microstructures from dispersions of silver salt solutions, as well as the fabrication of silver nanoparticle embedded microstructures by a combination of UV exposure and thermal curing. The last section summarizes the functionalization of semiconductor quantum dots for their incorporation into microstructures. These materials pave the way for new investigations into photonic properties of hybrid inorganic nanomaterial incorporated microstructures.

Keywords Nanomaterials; nanoparticles; photonics; quantum dots; silver; two-photon lithography

1. Introduction

Fabrication of microstructures containing high refractive index materials like noble metals and semiconductors is a challenging task in lithography. Clear high refractive index non-birefringent polymeric structures are crucial for photonic applications. High refractive index polymers are usually synthesized by incorporating inorganic materials [1–4]. Incorporation of inorganic nanomaterials into hierarchical polymeric microstructures can lead to a periodicity in refractive indices. Such a periodicity of high refractive indices is crucial for many photonic devices [5–8].

In this article we elaborate on the incorporation of silver nanomaterials as well as quantum dots (QDs) into microstructures using two-photon lithography. Two-photon lithography (TPL) is a maskless lithographic technique that relies on third-order nonlinear optical phenomena [9–11]. This technique is also called direct laser writing because it writes structures in photoactive media without any masking and realigning steps.

Silver nanoparticles are known for their outstanding optical properties. Silver has the highest light absorption cross-section of all known materials and shows high third-order

*Address correspondence to Kwang-Sup Lee. Tel.: +82-42-629-8857; Fax: +82-42-629-8854. E-mail: kslee@hnu.kr

nonlinear optical activity [12]. The prominence of plasmonic effect in silver nanoparticles (SNPs) make them favorites for studies in fields like surface enhanced Raman spectroscopy (SERS) and plasmonics. Silver ions are highly susceptible to reduction and they undergo reduction by accepting electrons from their surroundings [13]. At a sufficient concentration of silver, the reduced metal forms clusters and then nanoparticles, both of which act as templates for further reduction of silver on to them. Two different approaches are presented for structures involving silver nanomaterials namely direct writing of silver structures from dispersed silver salts and combined photo-thermal method for incorporation of SNPs into polymeric microstructures.

Quantum dots are semiconducting nanocrystals with unique optical and electrical properties due to their quantum confined size. Quantum dot containing polymeric composites finds application in optical data storage, photonic crystal fibers, photorefractivity and photodetection [14–16]. Quantum dots synthesized by conventional methods are not compatible with lithographic applications because of aggregation induced by long alkyl chains of stabilizing ligands. In our studies quantum dots were functionalized with photo-crosslinkable groups to make them compatible to organic media. This allows easy incorporation of QDs into polymerizable resins and fabrication of three-dimensional microstructures containing them.

Downloaded by [Renmin University of China] at 11:07 13 October 2013

2. Fabrication from Aqueous Solution of Silver Salts

A typical microfabrication system used for two-photon lithography consists of a mode-locked Ti:sapphire laser operating at 780 nm and 80 MHz with a pulse width of less than 100 fs. A high-numerical-aperture lens (NA = 1.4, with immersion oil) enables high-resolution three-dimensional addressing of points within the photopatternable materials. The patternable materials are placed on a cover glass fixed by a jig moved in x, y and z directions via piezoelectric stages [11, 17–20].

The easiest method for fabricating silver containing microstructures with TPL is direct reduction (direct writing) of silver structures from aqueous solution of its salt precursors. This is possible due to the high optical excitation and strong third-order nonlinear optical susceptibility $\chi^{(3)}$ of silver [21]. Although the reduction of silver from aqueous solutions is easy, the fabrication of well formed 1-, 2-, and 3-D structures from this process is not trivial. Direct writing involves laser induced formation of SNPs followed by their aggregation or melting-coalescence to form structures. The concerted and controlled effect of these phenomena would lead to well-formed microstructures. The formation of SNPs during direct writing would depend on the laser power, nature of the silver precursor and its dispersion. The melting-coalescing would depend on the size of the nanoparticles formed and the energy deposited by the laser. The mechanism governing the reduction of metals during direct writing of silver structures is quite different from two-photon induced photopolymerization (TPP). Radiolytic reduction of silver from aqueous as well as organic media is an extensively investigated phenomenon [22–25]. The aqueous reduction of silver can be briefly described as given below.

Radiolysis of water

$$H_2O \rightarrow H_2O^+ + e^-$$

$$e^- + H_2O \rightarrow H_2O^-(e^-_{aq})$$

$$H_2O^+ \rightarrow H^+ + OH$$

$$H_2O^- \rightarrow H + OH^-$$

Reduction of silver

$$Ag^{+}\, e^{-}_{aq} \rightarrow ag^{0}$$

$$Ag^{+} + H \rightarrow Ag^{0} + H^{+}$$

$$Ag^{0} + Ag^{+} \rightarrow Ag_{2}^{+}$$

$$Ag_{2}^{+} + Ag^{0} \rightarrow Ag_{3}^{+}$$

The $Ag_3{}^+$ silver clusters give rise to silver nanoparticles (SNPs) by catalyzing further reduction of silver ions. These SNPs either melt or aggregate to form nanostructures depending on the conditions or fabrication. Nanoparticles formed due to laser ablation lead to a number of non-linear optical processes in silver salt containing solutions like two-photon absorption, thermally induced self-defocusing and saturated absorption. At higher pulse rates the real part of third-order nonlinear optical susceptibility $|\mathrm{Re}\ \chi^{(3)}|$ dominates its imaginary counterpart $|\mathrm{Im}\ \chi^{(3)}|$ in case of SNP containing solutions. Since the real part accounts for scattering and the imaginary part accounts for nonlinear absorption, there is more scattering than non-linear absorption when there are a lot of SNPs in the fabrication medium [12].

The medium in which the metal salts are dispersed for direct writing of silver microstructures determines the local concentration of silver ions and hence the formation of SNPs due to laser induced reduction. Direct writing of silver microstructures has been reported from aqueous as well as polymer containing films or solutions [26–32]. In case of aqueous solutions the ions are free to flow about. The flow effects, the gradient in concentration of silver salts due to laser induced reduction, and thermal effects related to laser all govern the eventual shape and size of the fabricated structure.

The change in fabrication of line structures with energy and material conditions are demonstrated in Fig. 1. Aqueous solutions of silver nitrate of different concentrations were (0.1–0.3 M) used for direct writing of silver structures. Increase in concentration of silver salt solution had a marked effect in the formation of linear structures. Fig. 1(a) shows the line structures obtained from a 0.1 M aqueous solution of $AgNO_3$. The pattern was formed due to the aggregation of SNPs as seen in Fig. 1(b). The difference between line structure formed by a 0.1 M solution and a 0.2 M solution is seen in Fig. 1(c). Heating effects were found to deform the fabricated line structures. Heating effects in a structure fabricated from a 0.2 M aqueous solution of silver is seen in Fig. 1(c).

The formation of silver lines from aqueous solutions can be visualized as a process involving two steps; the first the formation of SNPs due to reduction of silver by the femtosecond laser followed by the aggregation, and/or melting of these nanoparticles to form line structures [26–28]. Short wavelength pulses when interacting with spherical SNPs give rise to prolate or oblate shaped nanoparticles [33]. These shapes can be clearly seen in Fig. 1(b). The shape change occurring in the SNPs formed by initial laser ablation would depend on factors like irradiation, pulse duration, intensity and number of pulses. The interaction of SNPs with laser would first lead to ultrafast electron and ion emission followed by a rapid increase in transient temperature [33]. The melting behavior of noble metals exhibit dramatic changes depending on the size of the nanoparticle [34–43]. In case of gold nanoparticles the melting point decreases considerably from the bulk value 1064°C depending on the size of the nanoparticle. This is due to the huge increase in the surface energy of nanoparticles, on going from 5 nm to 2 nm the melting point of gold nanoparticles decrease from ~827°C to 327°C. SNPs below 20 nm were found to melt and coalesce between 150–200°C [43]. Very high powers during TPL would lead to generation of larger nanoparticles which would form aggregates rather than melt to form continuous

Downloaded by [Renmin University of China] at 11:07 13 October 2013

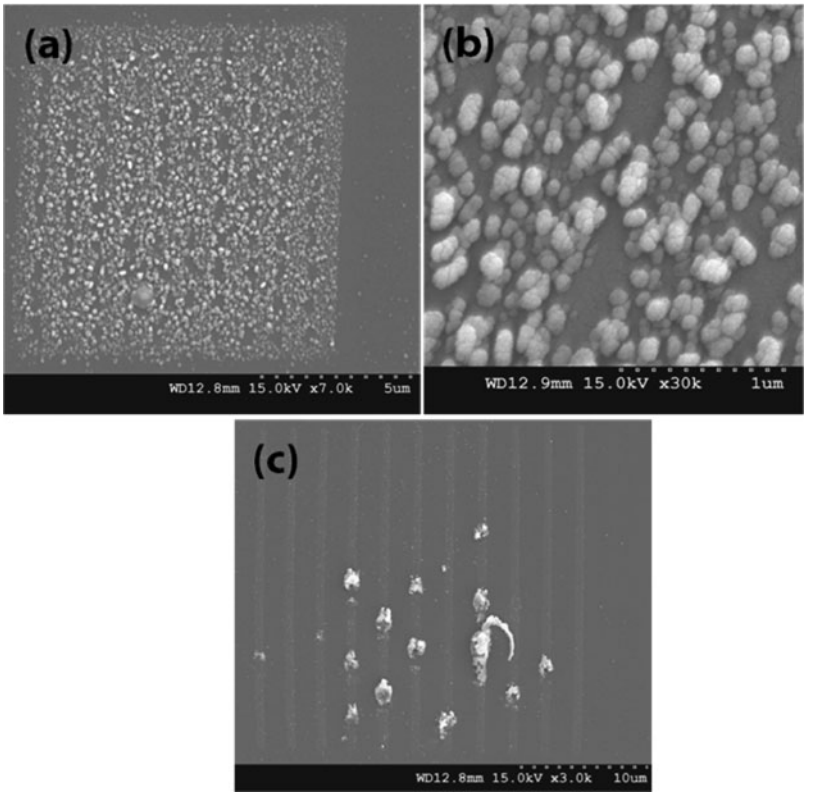

Figure 1. Silver reduction from aqueous solutions. (a) Line structure fabricated from 0.1 M aqueous solution of $AgNO_3$ at 120 mw with a laser scanning speed of 40 nm/ms. (b) Arrangement of SNPs formed from laser ablation of 0.1 M aqueous solution of $AgNO_3$. (c) Line structures fabricated by direct writing from 0.2 M silver solutions under the same laser parameters, the effects of laser induced heating of the fabricated structure can be seen in this figure.

Downloaded by [Renmin University of China] at 11:07 13 October 2013

nanostructures. This problem can be circumvented by aiding the formation of small SNPs at lower fabrication powers. To achieve this, the surface of the glass substate used for fabrication of metal microstructures was a modified by a self-assembled monolayer (SAM) layer of aminopropytrimethoxy silane (APTMS-SAM). The amino groups in aminopropyltriethoxy silane (APTES)-SAM will ligate to SNPs and help them adhere to the glass surface [44–46].

The silver precursor solution for fabrication was sonicated for 8 mins to generate SNPs of sizes around 8 nm. The time duration and power of the sonication process would govern the sizes of the SNPs [44, 47]. Aqueous silver nitrate solutions were sonicated for different periods of time with a 42 KHz ultrasonicator. The size of the SNPs was studied with dynamic light scattering experiment. It was found that the size of sonochemically formed silver SNPs increased steadily until 8 to 10 minutes and showed only gradual change thereafter. The analysis of the SNPs containing solutions gave the size of the nanoparticle at 10 minute about 8 nm. Very high surface energy of the dispersed SNPs aids ease of fabrication by reducing the threshold energy for microfabrication. In addition to these two measures a water soluble phenylene vinylene based TPA dye (PV1) was added to

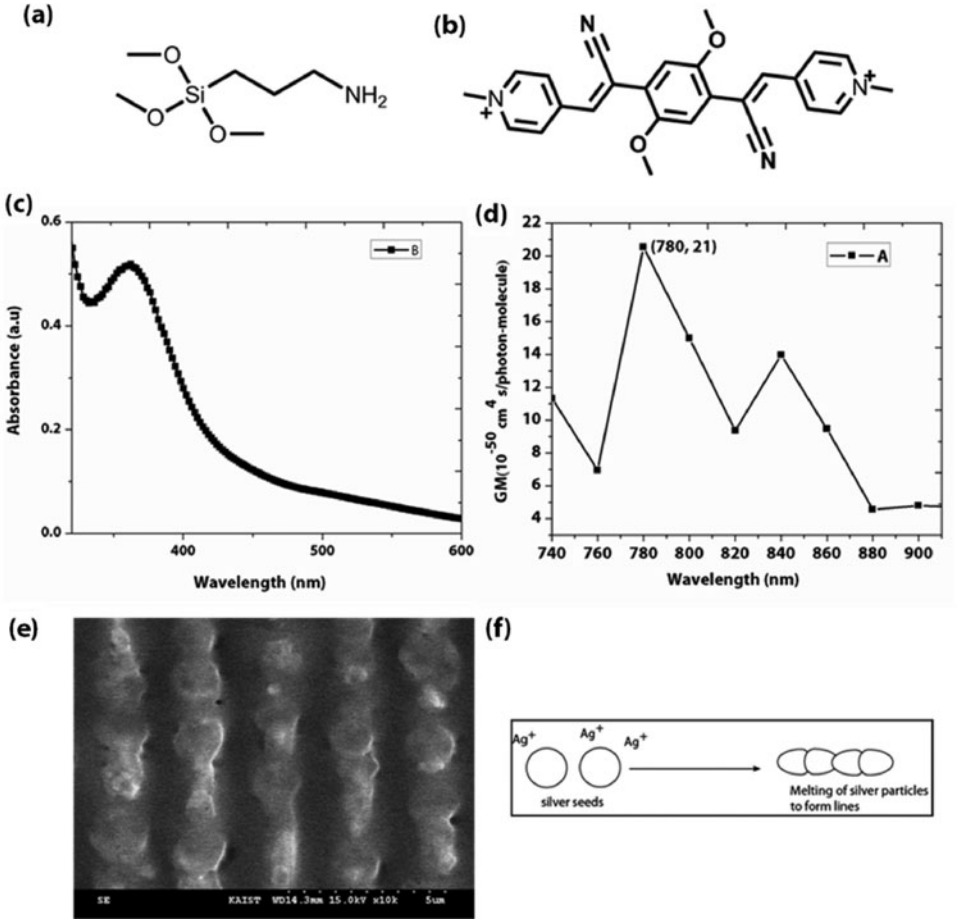

Figure 2. Improving reduction from aqueous solutions. (a) 3-Aminopropyltrimethoxysilane used for surface modification of glass substrates. (b) Water soluble TPA dye used for improving fabrication by reduction of power. (c) The UV absorption of the TPA dye. (d) The TPA absorption cross-section of the TPA dye. (e) Line structure fabricated from a 0.3 M aqueous solution of $AgNO_3$ that was sonicated to generate nanoparticle seeds and containing the TPA dye. (f) The proposed mechanism of formation of silver lines.

the fabrication solution to increase the two-photon sensitivity of the fabrication solution [48]. The structure of the silane coupling agent and the structure of PV1 can be seen in Fig. 2(a) and (b), respectively. The one-photon absorption characteristic of PV1 is given in Fig. 2(c) and its two-photon absoption cross section can be seen in Fig. 2(d). Using these improvements continuous lines could be fabricated with a 0.3 M solution of aqueous silver nitrate. The TPA dye was added in the amount of 0.1 wt% of the overall solution. Thick continuous lines could be fabricated from this solution at 120 mW power and exposure time of 1 ms. The above mentioned improvements in the fabrication solutions lead to more consistent results and reduced ablative effects. The fabricated lines can be seen in Fig. 2(e). Based on this we postulated that the mechanism of formation of lines follow the sequence shown in Fig. 2(f). The pre-reduced silver seeds play the role of a template for reduction

Downloaded by [Renmin University of China] at 11:07 13 October 2013

of silver on to them, the thermal coalescing of generated SNPs lead to formation of silver lines.

3. Fabrication from Silver Salts Dispersed in Aqueous Polyelectrolytes

Baldeck and co-workers introduced the use of polyelectrolytes as dispersion media for fabricating silver and gold microstructures through direct two-photon writing [29, 30]. Aqueous polyelectrolyte solutions when placed on a surface tend to self assemble when placed on a surface [49–51]. Silver nitrate (0.3 M) was dissolved in a 18 wt% solution of poly(styrenesulfonic acid)(PSSH). A drop of this solution easily forms a semi-solid film when placed on a glass plate surface modified with a SAM of 3-aminopropyl-trimethoxysilane. This film can be used for fabrication of one and 2-D microstructures. Two-dimensional structures fabricated from silver nitrate dissolved in PSSH containing aqueous solution can be seen in Fig. 3 (a)–(b) [52]. Subsequently a conductivity test was carried out on a silver wire structure fabricated between two gold pads (Fig. 3(c)). The log plot of observed current against applied voltage is shown in Fig. 3(d). The current characteristics show three different regions with region one showing very low currents. The current increases with the increase in voltage due to the increase in tunneling current between nanoparticles. The best conductivity values obtained were 3.18×10^4 S m^{-1} for region 3 which is about three orders of magnitude lower than bulk silver. These conductivity values are appropriate for applications such as RFID tags and OLEDs.

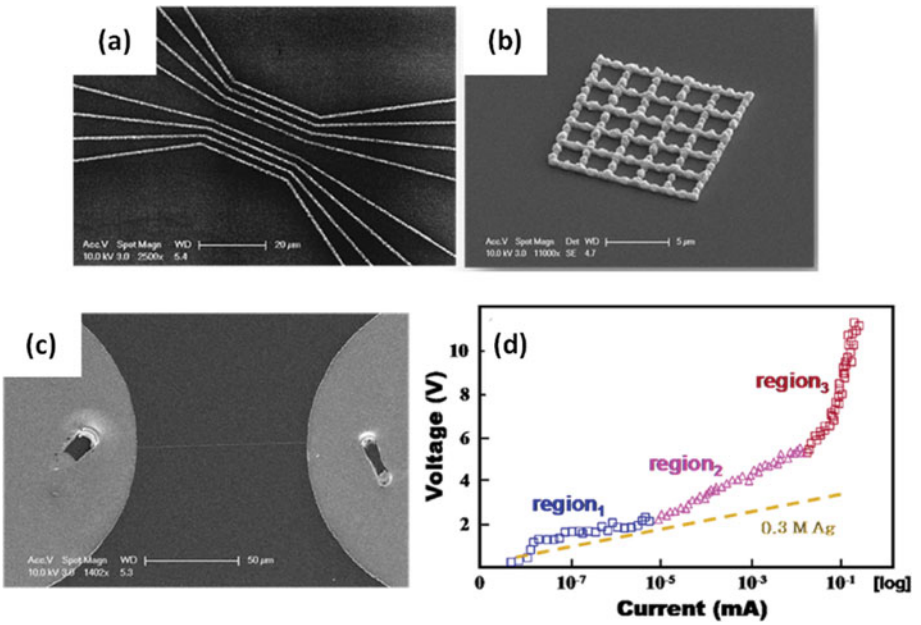

Figure 3. Two-dimensional microstructure fabricated from $AgNO_3$ dissolved in aqueous poly (styrene sulfonic acid) (18 wt%) solution. (a) Wire array [52]. (b) Mesh strucure. (c) Silver wire structure fabricated between two conductive pads for the electrical conductivity experiments. (d) Voltage plotted against log (current) for the wire structures.

Downloaded by [Renmin University of China] at 11:07 13 October 2013

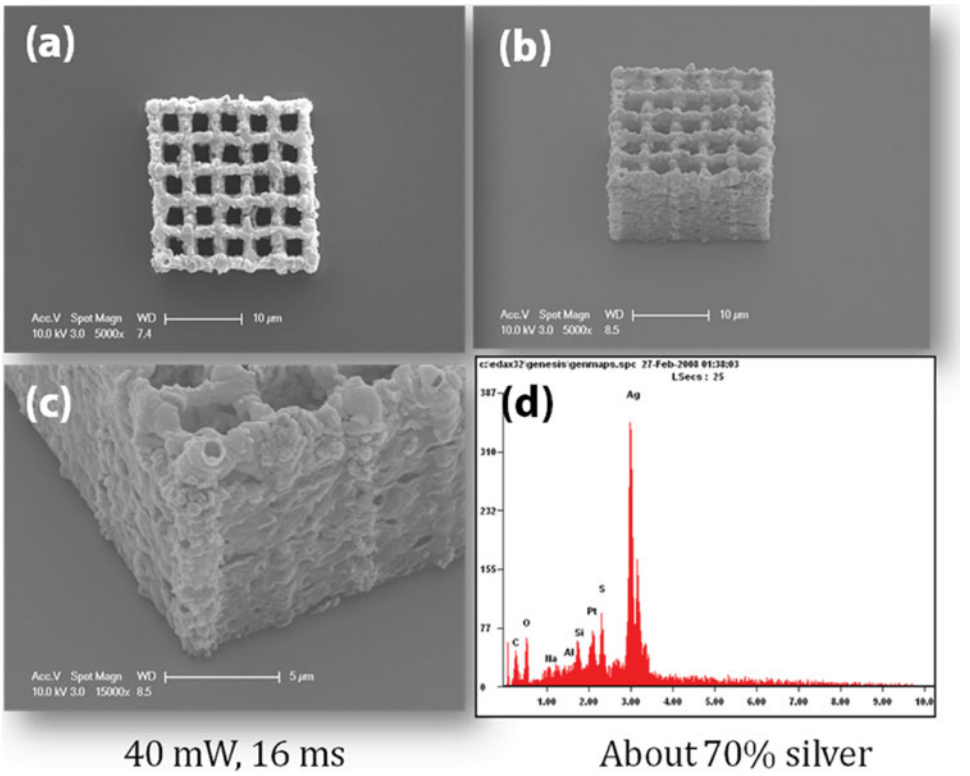

Figure 4. (a)–(c) Different views of three-dimensional metal structure created by direct writing of 2 M aqueous solutions of AgTFA in PSSH (18 wt%). (d) The silver content of the structure from EDS measurements.

The APTMS-SAM was not found to give satisfactory results when 3-D structures were fabricated on glass modified with it. Through trials the higher molecular weight 3-aminopropyltriethoxysilane was found to give most stable structures. Further to imporve the purity of fabricated structures silver nitrate was replaced by silver trifluoroacetate (AgTFA) as the silver source in fabrication solutions. AgTFA is widely used in matrix assisted laser desorption ionization time of flight (MALDI-TOF) mass spectrometry as a cationizing agent. It was seen from the investigation of silver ion background in MALDI experiments that in presence of polar matrices AgTFA could form silver clusters of large mass under suitable conditions of irradiation [53–56]. Similar effects cannot be ruled out under the conditions of two-photon direct writing of silver structures since there are possibilities of secondary emissions at lower wavelengths which can create MALDI like conditions. For the same fabrication conditions better structures with lesser surface roughness were achieved from solutions containing AgTFA. The combination of effective surface functionalization provided by APTES self-assembled layers with the AgTFA reduction from PSSH aqueous solution free standing silver 3-D structure could be fabricated, Fig. 4. From EDS measurements silver was found to have high silver content.

Downloaded by [Renmin University of China] at 11:07 13 October 2013

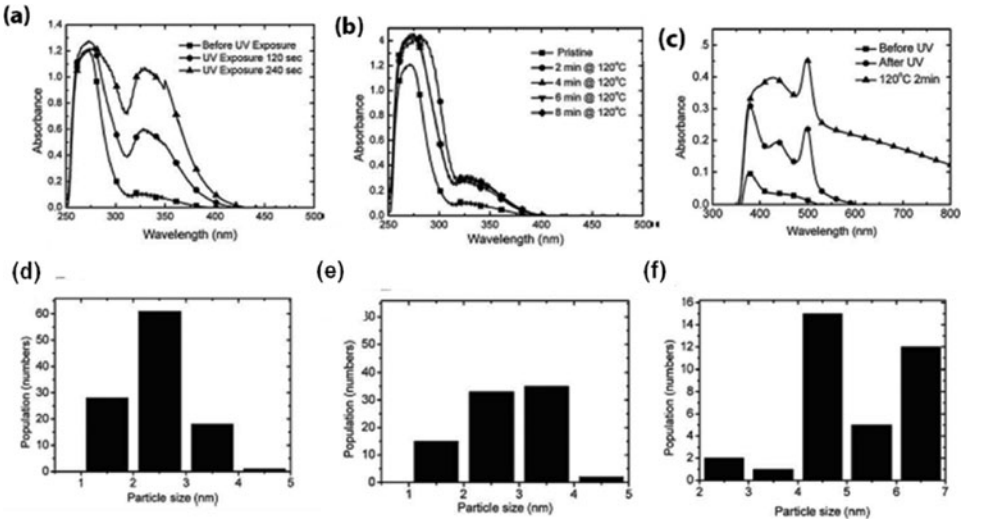

Figure 5. (a)–(c) Show the UV-Vis spectra of silver reduction in GBL solutions during photocuring, thermal curing as well as combination of photo and thermal curing in SU8 films. All spectra show surface plasmon peaks characteristics of SNPs. An increase in aspect ratio of nanoparticles shifts the absorption to the longer wavelength region. (d)–(f) Depicts the particle size distribution for photocuring in GBL, thermal curing in GBL and combined photo and thermal curing in GBL respectively [60].

4. Micorstructures Containing Silver Nanoparticles

Generation of silver nanoparticles from femtosecond laser ablation in various organic media has been well investigated before for fabrication of 3-D microstructures [12]. The main disadvantage of this method is that there can be laser induced heating with transient temperatures as high as 500 K in an area of few nanometers around the nanoparticle which negatively influence the fabrication of well formed microstructures [33]. To limit such deforming effects we adopted a combination of photo- and thermal-curing methods to generate uniformly distributed nanoparticles inside microstructure fabricated using the epoxy resin SU8.

Silver trifluoroacetate is used as the precursor silver salt for *in-situ* generation of silver nanoparticles inside microstructure. Fluoroacetates are generally considered to be good for depositing silver layers through thermal reduction due to their high thermal stability [57–59]. In a typical experiment, SU 8 resin contains about 2 wt% triphenylsulfonium hexafluoroantimonate photoacid generator (PAG). A highly active spirofluorene-based two-photon absorbing (TPA) dye 3,6-bis(3,7-dimethyloctyloxy)-2,7-diphenyl-(4-vinylphenyl)amine-9,9′-spirobifluorene (TP-MOSF-TP) (0.1 wt%) was added as two-photon photosensitizer in the SU 8 resin [60]. The TPA dye acts as a sensitizer by first absorbing two-photon at focus of the laser and then transferring the energy to the PAG through de-excitation or through photoinduced chemical reactions. The acid generated by the PAG will initiate the cationic ring opening polymerization in epoxy resin. Initial studies involved seperate experiments aimed at studying the the UV induced reduction of silver from AgTFA solutions in γ-butyrolactone (GBL) as well as thermal reduction of AgTFA (3 wt%) solutions in GBL. The UV spectra of SNPs generated by UV and thermal curing of AgTFA solutions in GBL are summarized in Fig. 5(a) and (b), respectively. The corresponding particle size distributions are given in Fig. 5(d) and (e).

Downloaded by [Renmin University of China] at 11:07 13 October 2013

Downloaded by [Renmin University of China] at 11:07 13 October 2013

Irradiation of solutions leads to the formation of electrons which then reduce the silver ions to form silver clusters. These silver clusters act as catalysts for further reduction and eventually lead to the formation of nanoparticles. The effect of UV irradiation time on silver reduction in GBL solutions is clearly reflected on the absorption spectrum of samples as shown in Fig. 5(a). Compared to unexposed solution, solutions exposed for 120 and 240 seconds, show an absorption around 265 nm, followed by growth of absorption at 325 nm, may be due to the formation of silver clusters like Ag^{2+} and $Ag_4{}^0$, respectively. For solution exposed for 240 seconds, a small absorption at 360 nm can be seen, which can be attributed to the formation of $Ag_1{}^0$ [24, 61, 62]. On increasing the exposure time the surface plasmon peak can be seen increasing at 325 nm. The difference in peak intensity on going from 120 to 240 seconds exposure time is attributed to increasing number of particles and not increasing particle size. An increase in the aspect ratio of the particle is expected to shift the absorption towards longer wavelength [12]. These observations are in agreement with particle size distribution measurement of the UV irradiated solution shown in Fig. 5(d). Large number of nanoparticle nucleates with 2.5 ± 1.0 nm particle size were found in the solution, from transmission electron microscopy the particle density was measured to be 0.067 nm^{-2}.

The results of thermal curing of AgTFA in GBL solutions with same concentration for varying periods at a temperature of 120°C, are shown in Fig. 5 (b) and (e). The UV spectrum shifted towards longer wavelengths (Fig. 5 (e)), with increase in thermal treatment time due to the formation of particles with larger aspect ratio. There was a reduction in the number of smaller nucleates due to the coalescing growth to form larger particles. The average particle size is calculated to be 3.1 ± 1.2 nm with a density 0.050 nm^{-2}.

In order to study the effect of combined photo and thermal curing, we conducted experiments with SU 8 resin containing 8 wt% AgTFA and the results are summarized in Fig. 5(c) and (f). During the photocuring step the photoacid is generated initiating the polymerization which is completed only during the thermal (post) curing step. Both the photo and thermal curing steps are required to complete the polymerization; photocuring (4 mins) initiated the nucleation of SNPs, followed by thermal curing at 120°C (2 mins) lead to diffusion growth of nanoparticle, which resulted in the broadening of the UV absorption. The average particle size was 4.4 ± 2.0 nm and the density of particles is 0.029 nm^{-2}.

Fabrication experiments were then conducted with various concentrations of AgTFA in SU 8 resin containing 0.1 wt% TPA dye. During two-photon direct laser writing a three-dimensional latent image of the structure is generated through photoacid generation. The actual structure is formed during a post baking step due to cationic polymerization of SU8 [63, 64]. An excess of silver salts in the fabrication medium can lead to large scale generation of SNPs which would then hamper proper crosslinking of the epoxy networks during post curing.

The results from a fabrication experiment involving 2 wt% AgTFA can be seen in Fig. 6(a). The final structure is misformed and collapsed around SNPs. The energy dispersive spectroscopy of structure with 2 wt% AgTFA shows a very high silver content (Fig. 6(b)). The number of initiating species generated during two-photon polymerization is about two orders of magnitude greater than that in one-photon polymerization [65]. Hence the concentration of silver used to generate nanoparticles in polymeric structures should be less than that required in the case of conventional patterning [60]. In our study, we found that 0.2 wt% silver salt mixed SU 8 resin three dimensional structures with uniform distribution of SNPs could be generated. A three dimensional structure embedded with SNPs could be seen in Fig. 6(c), a close-up image of the nanostructure is shown in Fig. 6(d). Nanoparticles on the surface of the microstructure can be clearly seen discerned from the close up SEM

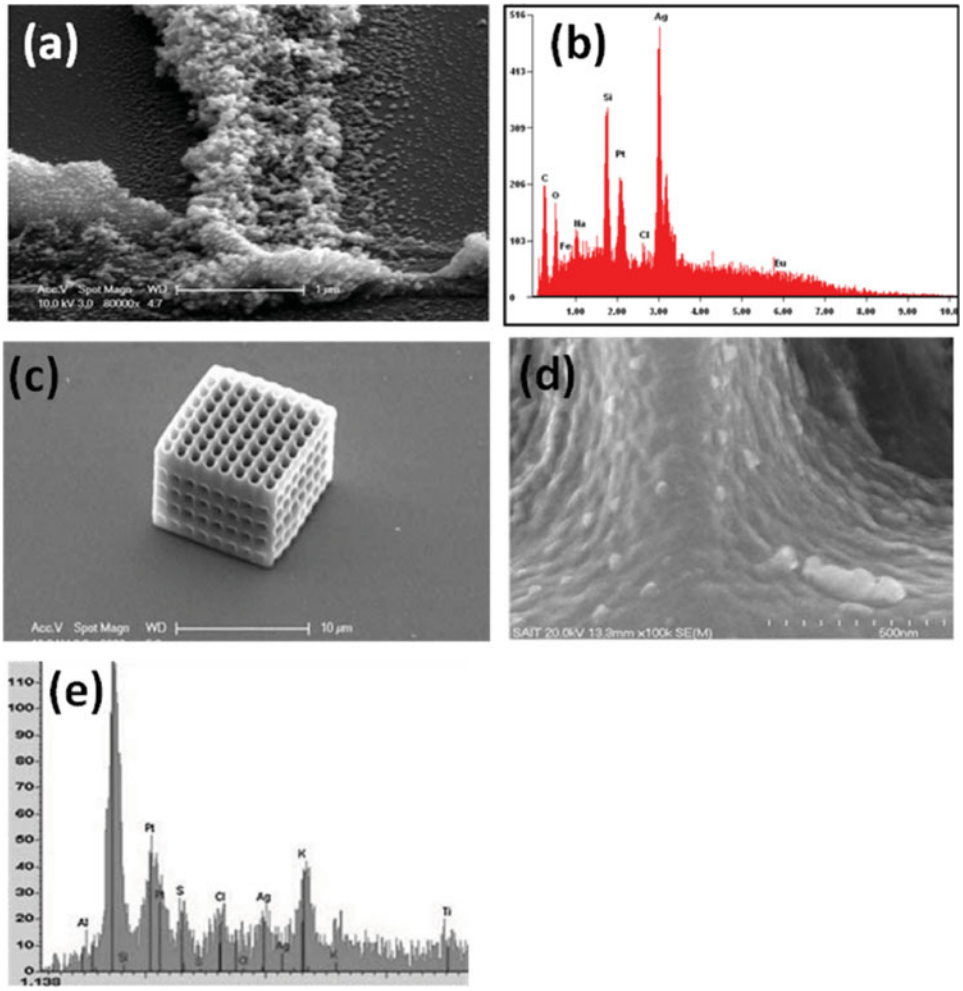

Figure 6. (a)–(c) Show the effect of concentration of silver salts in photopatternable resins. (a) A structure fabricated by a resin containing 2 wt% AgTFA. The structure is destabilized by the heating effect due to interaction of photoreduced SNPs with laser. The EDX spectrum of the structure fabricated from resin containing 2 wt% silver salt is seen in (b). (c) 3-D structure fabricated with a resin containing 0.2 wt% AgTFA. (d) Close up showing nanoparticles embedded in the fabricated three-dimensional woodpile structure. (e) EDX spectrum of the microstructure surface. Reprinted with permission from the Wiley-VCH Verlag [60].

image of the surface of a woodpile structure. The presence of silver is confirmed from the energy dispersive X-ray (EDX) analysis of the surface of the structure given in Fig. 6(e).

5. Quantum Dot Embedded Microstructures

Some research groups have attempted the fabrication of microstructures containing QDs through either direct mixing of QDs with polymerizable precursor or *in situ* generation of QDs inside microstructures [66, 67]. The former method leads to aggregation of QDs while the latter results in a polydisperse lot of semiconductor nanocrystals. To overcome these

Downloaded by [Renmin University of China] at 11:07 13 October 2013

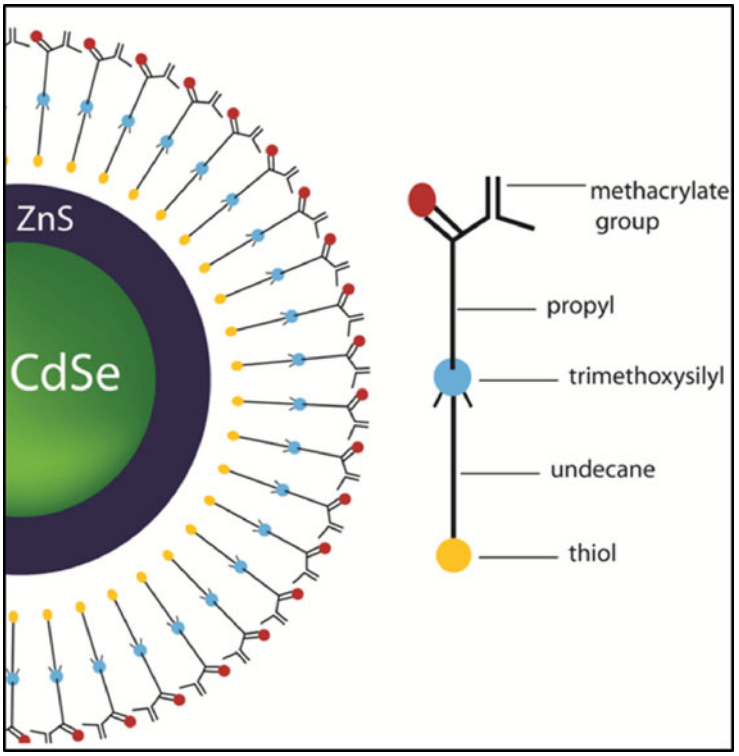

Figure 7. Photopatternable quantum dots used in our study. The thiol group anchors to the CdSe/ZnS nanoparticle surface, the siloxane group can undergo thermal crosslinking to provide an additional passivation layer. The methacrylate group could be photocrosslinked.

issues we developed QDs with photopatternable functionalization [68]. The CdSe/ZnS core-shell QD was synthesized following reported procedure [69], the QD with photopatternable functionalization is shown in Fig. 7. The stabilizing ligand consist of thiol group for anchoring onto CdSe/ZnS core shell quantum dots, and inner siloxane layer capable of thermal crosslinking to provide an additional passivation layer. The terminal methacrylate group capable of photocrosslinking facilitates the easy patterning of QDs.

In a typical experiment, 2 ml of photofunctionalized QDs (1.125 mg/ml in ethanol) is mixed well with 1 ml urethane acrylate resin SCR 500, filtered, and the excess of solvent was removed by slow evaporation under vacuum at low temperatures.

The dye TP-MOSF-TP was added to the QD dispersed resin before fabrication of 2- and 3-D microstructures with two-photon stereolithography. Scanning electron microscopy (SEM) and confocal microscopy were used to verify the incorporation of nanoparticles into the polymer matrix through polymerization and the images of various planes of the microfabricated structure are summarized in Fig. 8(a)–(e). For comparison, SEM image and confocal image of a 2-D map of the Korean peninsula are given in Fig. 5(a) and (b), respectively. Fig. 5 (c) and (d) correspond to TEM and confocal images of a 3-D woodpile structures, respectively. Fig. 5(e) gives the rotated image of a woodpile structure generated by stacking the confocal images of different layers of that structure, which clearly demonstrates the high yield monodisperse QDs inside the structure.

Downloaded by [Renmin University of China] at 11:07 13 October 2013

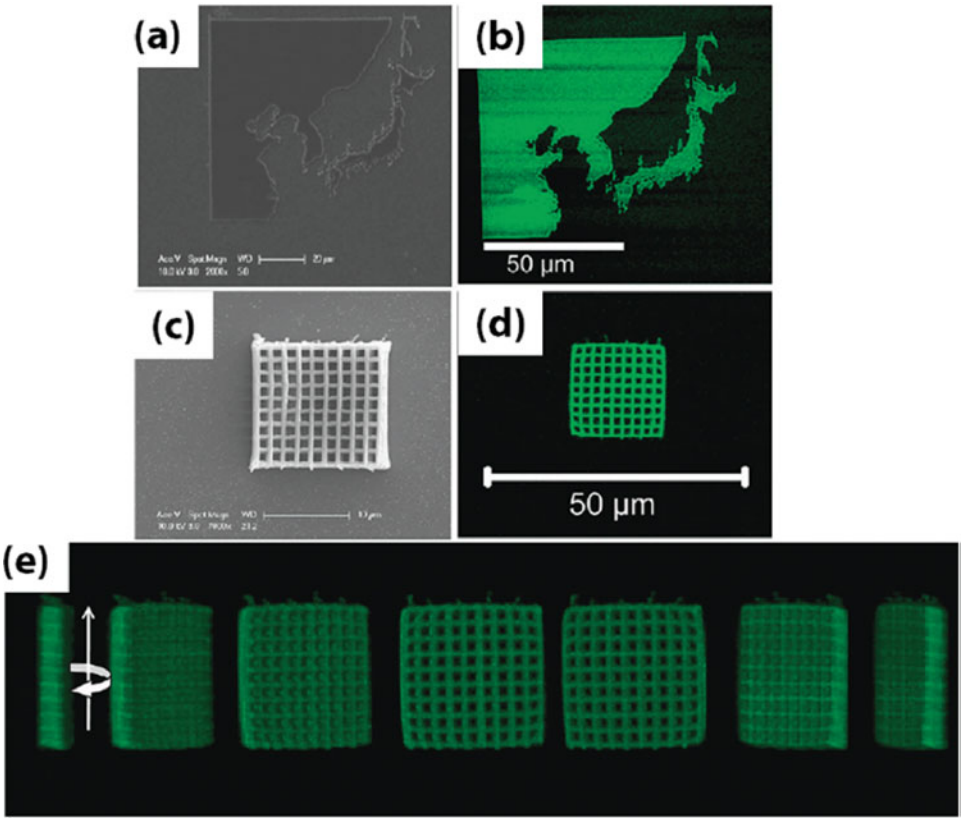

Figure 8. 2-D and 3-D structures fabricated by quantum dot dopped photopatternable resins. (a) SEM images of a 2-D Map structure (scale 20 μm). (b) Confocal microscopy images of the same structure (scale 50 μm). (c) SEM image of 3-D woodpile structure (scale 10 μm). (d) The corresponding confocal microscopy images (scale 50 μm). (e) A rotated image of a z-stach of different planes of the woodpile structure imaged by confocal microscopy. This demonstrates the uniform incorporation of QDs inside the resins. Reprinted with permission from American Chemical Society [68].

6. Conclusion

The non-linear nature of TPL facilitates easy fabrication of complex microstructures without involving any time consuming masking techniques. If the versatility of this process could be proved for structuring different materials it could provide a cheap alternative to many coventional lithographic techniques. This was our primary motivation towards developing materials and methods for silver and semiconductor quantum dot containing microstructures. We have investigated the effect of varying material content on the dimensionality and shape of the structures obtained by direct laser writing of silver precursor solutions. The dispersion of silver precursor uniformly in the fabrication solution as well as surface functionalization of the substrate was found to be crucial for the fabrication of three-dimensional silver microstructures. To fabricate silver nanoparticle embedded microstructures we have evolved a photo-thermal curing method. This method was found to be appropriate in by passing the adverse heating effects due to formation of large SNPs

Downloaded by [Renmin University of China] at 11:07 13 October 2013

during direct writing of microstructures. Stable three-dimemsional silver nanparticle embdedded microstructures could be fabricated using this combinaton. Quantum dots were incorporated intro three-dimensional microstructures by evolving photo-crosslinkable surface functionalization. This was found to be very effective in increasing the dispersibility of QDs in organic media for photopatterning. Through this works we have strived to demonstrate that incroporation of high refractive index materials like noble metal nanoparticles and QDs in nanostructures could be improved and perfected by controlling the chemistry of precursor materials.

Acknowledgment

This work was supported by the National Research Foundation (NRF) grant funded by the Korea government (MEST) through the Active Polymer Center for Pattern Integration (No. R11-2007-050-01001).

Downloaded by [Renmin University of China] at 11:07 13 October 2013

References

[1] Lee, L. H., & Chen, W. C. (2001). *Chem. Mater.*, *13*, 1137.
[2] Lü, C., Guan, C., Liu, Y., Cheng, Y., & Yang, B. (2005). *Chem. Mater.*, *17*, 2448.
[3] Lü, C., Cui, Z., Li, Z., Yang, B., & Shen, J. (2003). *J. Mater. Chem.*, *13*, 526.
[4] Chang, C. C., & Chen, W. C. (2001). *J. Polym. Sci. A1*, *39*, 3419.
[5] Schilling, J. (2011). *Nat. Photon.*, *5*, 449.
[6] You, B., Lu, J. Y., Yu, C. P., Liu, T. A., & Peng, J. L. (2012). *Opt. Exp.*, *20*, 5858.
[7] Brozell, A. M., Muha, M. A., Abed-Amoli, A., Bricarello, D., & Parikh, A. N. (2007). *Nano Lett.*, *7*, 3822.
[8] Colvin, V. L., Schlamp, M. C., & Alivisatos, A. P. (1994). *Nature*, *370*, 354.
[9] Kawata, S., & Kawata, Y. (2000). *Chem. Rev.*, *100*, 1777.
[10] Kawata, S., Sun, H. B., Tanaka, T., & Takada, K. (2001). *Nature*, *412*, 697.
[11] Lee, K.-S., Kim, R. H., Yang, D.-Y., & Park, S. H. (2008). *Prog. Polym. Sci.*, *33*, 631.
[12] Ganeev, R., Baba, M., Ryasnyansky, A., Suzuki, M., & Kuroda, H. (2004). *Opt. Commun.*, *240*, 437.
[13] Cuccureddu, F., Murphy, S., Shvets, I. V., Porcu, M., & Zandbergen, H. W. (2008). *Nano Lett.*, *8*, 3248.
[14] Alivisatos, A. P. (1996). *Science*, *271*, 933.
[15] Bailey, R. E., Smith, A. M., & Nie, S. (2004*). Physica E*, *25*, 1.
[16] Xia, Y., Yang, P., Sun, Y., Wu, Y., Mayers, B., Gates, B., Yin, Y., Kim, F., & Yan, H. (2003). *Adv. Mater.*, *15*, 353.
[17] Lee, K. S., Yang, D. Y., Park, S. H., & Kim, R. H. (2006). *Polym. Adv. Tech*, *17*, 72.
[18] Lee, K.-S., Kim, R. H., Prabhahakaran, P., Yang D.-Y., Lim, T. W., & Park, S. H. (2007). *J. Nonlinear Opt. Phys.*, *16*, 59.
[19] Park, S. H., Lim, T. W., Yang, D. Y., Kong, H. J., & Lee, K.-S. (2005). *J. Korean Chem. Soc.*, *49*, 292.
[20] Pham, T. A., Kim, D. P., Lim, T. W., Park, S. H., Yang, D. Y., & Lee, K.-S. (2006). *Adv. Funct. Mater.*, *16*, 1235.
[21] Moskovits, M. (1985). *Rev. Mod. Phys.*, *57*, 783.
[22] Mahlman, H. A., & Willmarth, T. E. (1964). *Nature*, *202*, 590.
[23] Temgire, M., & Joshi, S. (2004). *Radiat. Phys. Chem.*, *71*, 1039.
[24] Ershov, B., Janata, E., Henglein, A., & Fojtik, A. (1993). *J. Phys. Chem.*, *97*, 4589.
[25] Ershov, B. G., Janata, E., & Henglein, A. (1996). *Radiat. Phys. Chem.*, *47*, 59.
[26] Cao, Y. Y., Takeyasu, N., Tanaka, T., Duan, X. M., & Kawata, S. (2009). *Small*, *5*, 1144.
[27] Ishikawa, A., Tanaka, T., & Kawata, S. (2006). *Appl. Phys. Lett.*, *89*, 113102.
[28] Tanaka, T., Ishikawa, A., & Kawata, S. (2006). *Appl. Phys. Lett.*, *88*, 081107.

[29] Tosa, N., Bosson, J., Pierre, M., Rambaud, C., Bouriau, M., Vitrant, G., Stéphan, O., Astilean, S., & Baldeck, P. L. (2006). *Proc. SPIE*, 619501.
[30] Vitrant, G., Bosson, J., Tosa, N., Rosenzveig, T., Stephan, O., Astilean, S., & Baldeck, P. L. (2007). *Proc. SPIE*, 647000.
[31] Stellacci, F., Bauer, C. A., Meyer-Friedrichsen, T., Wenseleers, W., Alain, V., Kuebler, S. M., Pond, S. J. K., Zhang, Y., Marder, S. R., & Perry, J. W. (2002). *Adv. Mater.*, *14*, 194.
[32] Tsutsumi, N., Nagata, K., & Sakai, W. (2011). *Appl. Phys. A-Mater.*, *103*, 421.
[33] Stalmashonak, A., Unal, A. A., Graener, H., & Seifert, G. (2009). *J. Phys. Chem. C*, *113*, 12028.
[34] Iijima, S., & Ichihashi, T. (1986). *Phys. Rev. Lett.*, *56*, 616.
[35] Ercolessi, F., Andreoni, W., & Tosatti, E. (1991). *Phys. Rev. Lett.*, *66*, 911.
[36] Bilalbegovic, G. (2000). *Solid State Commun.*, *115*, 73.
[37] Shim, J.-H., Lee, B.-J., & Cho, Y. W. (2002). *Surf. Sci.*, *512*, 262.
[38] Gibbs, D., Ocko, B. M., Zehner, D. M., & Mochrie, S. G. J. (1990). *Phys. Rev. B*, *42*, 7330.
[39] Dick, K., Dhanasekaran, T., Zhang, Z., & Meisel, D. (2002). *J. Am. Chem. Soc.*, *124*, 2312.
[40] Buffat, P., & Borel, J. P. (1976). *Phys. Rev. A*, *13*, 2287.
[41] Liu, H. B., Ascencio, J. A., Perez-Alvarez, M., & Yacaman, M. J. (2001). *Surf. Sci.*, *491*, 88.
[42] Kan, C., Wang, G., Zhu, X., Li, C., & Cao, B. (2006). *Appl. Phys. Lett.*, *88*, 071904.
[43] Okada, I., Shimoda, K., & Miyazaki, K. (2006). *SEI Technical Reviw*, 55.
[44] Pol, V. G., Srivastava, D. N., Palchik, O., Palchik, V., Slifkin, M. A., Weiss, A. M., & Gedanken, A. (2002). *Langmuir*, *18*, 3352.
[45] Ramanath, G., Cui, G., Ganesan, P., Guo, X., Ellis, A. V., Stukowski, M., Vijayamohanan, K., Doppelt, P., & Lane, M. (2003). *Appl. Phys. Lett.*, *83*, 383.
[46] Ferguson, G. S., Chaudhury, M. K., Sigal, G. B., & Whitesides, G. M. (1991). *Science*, *253*, 776.
[47] Salkar, A. R., Jeevanandam, P., Aruna, S. T., Koltypin, Y., & Gedanken, A. (1999). *J. Mater. Chem.*, *9*, 1333.
[48] Prabhakaran, P., Zur Borg, L., Son, Y., Domanski, A., Ha, C.-W., Zentel, R., Berger, R., Yang, D.-Y., and Lee, K.-S. *Unpublished results*
[49] He, G. S., Xu, G. C., Prasad, P. N., Reinhardt, B. A., Bhatt, J. C., & Dillard, A. G. (1995). *Opt. Lett.*, *20*, 435.
[50] Yu, B., Zhu, C., & Gan, F. (2000). *Physica E*, *8*, 360.
[51] Sheik-Bahae, M., Said, A. A., Wei, T. H., Hagan, D. J., & Van Stryland, E. W. (1990). *IEEE J. Quantum. Elect., 26*, 760.
[52] Son, Y., Lim, T. W., Yang, D. Y., Prabhakaran, P., Lee, K. S., Bosson, J., Stephan, O., & Baldeck, P. (2010). *Int. J. Nanomanufacturing*, *6*, 219.
[53] Rashidzadeh, H., & Guo, B. (1999). *Chem. Phys. Lett.*, *310*, 466.
[54] Negres, R. A., Hales, J. M., Kobyakov, A., Hagan, D. J., & Van Stryland, E. W. (2002). *IEEE J. Quantum. Elect.*, *38*, 1205.
[55] Hales, J. M., Hagan, D. J., Van Stryland, E. W., Schafer, K. J., Morales, A. R., Belfield, K. D., Pacher, P., Kwon, O., Zojer, E., & Bredas, J. L. (2004). *J. Chem. Phys.*, *121*, 3152.
[56] Parthenopoulos, D. A., & Rentzepis, P. M. (1989). *Science*, *245*, 843.
[57] Tsiminis, G., Ribierre, J. C., Ruseckas, A., Barcena, H. S., Richards, G. J., Turnbull, G. A., Burn, P. L., & Samuel, I. D. W. (2008). *Adv. Mater*, *20*, 1940.
[58] Lu, Y. F., Takai, M., Nagatomo, S., Kato, K., & Namba, S. (1992). *Appl. Phys. A- Mater.*, *54*, 51.
[59] Szlyk, E., Piszczek, P., Chaberski, M., & Golinski, A. (2001). *Polyhedron*, *20*, 2853.
[60] Park, J. J., Bulliard, X., Lee, J. M., Hur, J., Im, K., Kim, J. M., Prabhakaran, P., Cho, N., Lee, K. S., & Min, S. Y. (2010). *Adv. Funct. Mater.*, *20*, 2296.
[61] Ershov, B. G., Janata, E., & Henglein, A. (1996). *Radiat. Phys. Chem.*, *47*, 59.
[62] Ershov, B. G., Janata, E., & Henglein, A. (1993). *J. Phys. Chem.*, *97*, 339.
[63] Teh, W. H., Dürig, U., Drechsler, U., Smith, C. G., & Güntherodt, H. J. (2005). *J. Appl. Phys.*, *97*, 054907.

Downloaded by [Renmin University of China] at 11:07 13 October 2013

[64] Teh, W. H., Dürig, U., Salis, G., Harbers, R., Drechsler, U., Mahrt, R. F., Smith, C. G., & Güntherodt, H. J. (2004). *Appl. Phys. Lett.*, *84*, 4095.
[65] Leatherdale, C. A., & DeVoe, R. J. (2003). *Proc. SPIE*, 113.
[66] Jun, S., Jang, E., Park, J., & Kim, J. (2006). *Langmuir*, *22*, 2407.
[67] Sun, Z. B., Dong, X. Z., Chen, W. Q., Nakanishi, S., Duan, X. M., & Kawata, S. (2008). *Adv. Mater.*, *20*, 914.
[68] Park, J. J., Prabhakaran, P., Jang, K. K., Lee, Y. G., Lee, J., Lee, K. H., Hur, J., Kim, J. M., Cho, N., & Son, Y. (2010). *Nano Lett.*, *10*, 2310.
[69] Bae, W. K., Char, K., Hur, H., & Lee, S. (2008). *Chem. Mater.*, *20*, 531.

Downloaded by [Renmin University of China] at 11:07 13 October 2013